

SOME IMPROVEMENTS OF A ROTATION INVARIANT AUTOREGRESSIVE METHOD. APPLICATION TO THE NEURAL CLASSIFICATION OF NOISY SONAR IMAGES

H. Thomas[†] C. Collet[†] K. Yao[†] G. Burel[•]

[†] Ecole Navale, Groupe de Traitement du Signal, Bât. des Laboratoires, Lanvéoc-Poulmic
29240 Brest-Naval France, email : name@ecole-navale.fr

[•] Université de Brest, Département d'Electronique, 6 av. V. Le Gorgeu, BP 809
29285 Brest Cedex, France, email : burel@lest-gw.univ-brest.fr

ABSTRACT

This paper presents some improvements of a rotation invariant method based on Autoregressive (AR) 2D Models to classify textures. The basic model and our improved version are applied to natural sidescan sonar images (with multiplicative noise) in order to extract a reduced set of relevant rotation invariant features which are then used to feed a MultiLayer Perceptron (MLP) for identification task. The basic method provides three AR parameters, estimated over a 3×3 pixel neighbourhood. We propose an extension of this method to a 5×5 pixel neighbourhood in order to take spatial interactions into account more efficiently. Three new features are estimated. Some analyses are conducted over these features to evaluate their interest. Classification results on four types of sidescan sonar images illustrate the efficiency of the proposed approach.

1 INTRODUCTION

The classification of seafloor areas has two applications : the cartography of seafloors and the improvement of detection/classification steps of manufactured objects lying on these seafloors. A sonar image is formed by two types of areas: *shadow areas* which are due to the lack of reverberation and *seafloor areas* which characterize the signal reverberation on the bottom.

The key step of a recognition system lies in the appropriate feature calculation. Sonar images are highly textured and very noisy. Good reviews on texture analysis methods are given in [4][15]. The Grey Level Cooccurrence Method (GLCM) [5] and the Run Lengths Method [2] are widely used in satellite imagery [9][11] or in sidescan sonar imagery [12][13]. Other approaches concern the Gibbs Random Field Models [1], the Gabor filters [3] and the Autoregressive (AR) models [6][7].

We are specially interested in 2D AR rotation invariant modelisation reported in [7] for the four following advantages: 1) spatial interactions are efficiently taken into account; 2) AR rotation-dependent models presented in [6] have shown good classification results on our sonar images; 3) the method is rotation invariant and seems to be efficient; 4) a reduced number of relevant features is provided by this method.

To improve the efficiency of the rotation invariant AR method, we introduce three additional AR similar parameters which describe a larger neighbourhood. Spatial interactions are then better taken into account. Other studies in the fields of Markov Random Fields [10] and AR Models [8] have shown the interest of extending the neighbourhood size.

An MLP is used to perform identification tasks. A K-Nearest Neighbour Algorithm is also used for comparison.

This paper is organized as follows : the method and its improvement are described in section 2 whereas feature analysis is given in section 3. The 4th section illustrates the efficiency of the improved method applied to four types of natural sidescan sonar images (with multiplicative noise): pebbles, dunes, ridges and sand (see Figure 1). Finally, it gives some comparative results.

2 MODELS AND FEATURE ESTIMATION

2.1 Basic Model

Let be I a $M \times M$ image and $\{y(p), p = (p_1, p_2) \in \Omega\}$ the set of pixel intensities where $\Omega = \{0 \leq p_1, p_2 \leq M - 1\}$. The first model applied to image I is described by the following equation:

$$y(p) = \alpha_{11} \sum_{n \in N_c} y(p+n) + \sqrt{\beta_{11}} \cdot v(p) \quad p \in \Omega \quad (1)$$

where $N_c = \{(0, 1), (0, -1), (1, 0), (-1, 0), (\sqrt{2}/2, \sqrt{2}/2), (-\sqrt{2}/2, -\sqrt{2}/2), (\sqrt{2}/2, -\sqrt{2}/2), (-\sqrt{2}/2, \sqrt{2}/2)\}$, N_c is called circular neighbourhood and $v(p)$ is a correlated sequence with zero mean and unit variance. The parameter α_{11} and the roughness parameter β_{11} are estimated by a Least Square (LS) approach. See [7] for details about the interpolation of neighbourhood pixel intensities and the LS estimation. The following model is then used twice to calculate the third parameter ζ_{11} called directional parameter:

$$y(p) = \sum_{n \in N_d} \theta_n y(p+n) + \sqrt{\rho} \cdot w(n) \quad p \in \Omega \quad (2)$$

where N_d is a neighbourhood set and $\{\theta_n, n \in N_d\}$ the set of AR parameters attached to N_d . In a recent study [14], we established that $\theta_n^* = \theta_{-n}^*$, where θ_n^* are θ_n LS-estimates. So, unlike [7] we first use $N_d = \{(0, 1), (1, 0)\}$ and then $N_d = \{(1, 1), (-1, 1)\}$. Finally, the directional parameter ζ_{11} is given by:

$$\zeta_{11} = \max\{|\theta_{(1,0)} - \theta_{(0,1)}|, |\theta_{(1,1)} - \theta_{(-1,1)}|\} \quad (3)$$

2.2 Improved Model

The neighbourhood considered in the last section is restricted to 3×3 pixels. The directions taken into account to estimate ζ_{11} are 0, 45, 90 and 135 degrees. We have noted that a 5×5 pixel neighbourhood is required to obtain good classification results. So we propose to adapt and improve

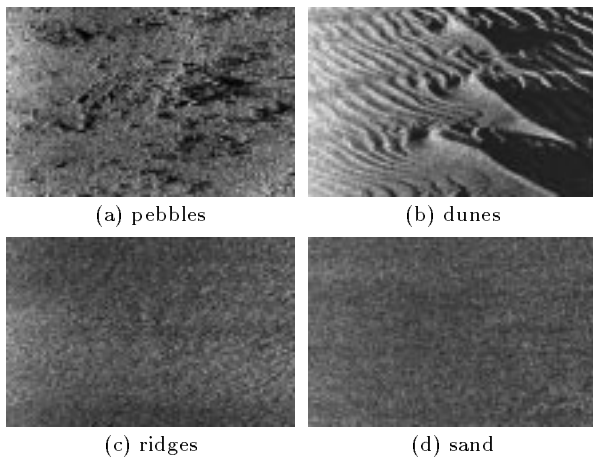


Figure 1: Four types of seafloors (512×768 pixels). One pixel represents about 100 cm² on the seafloor.

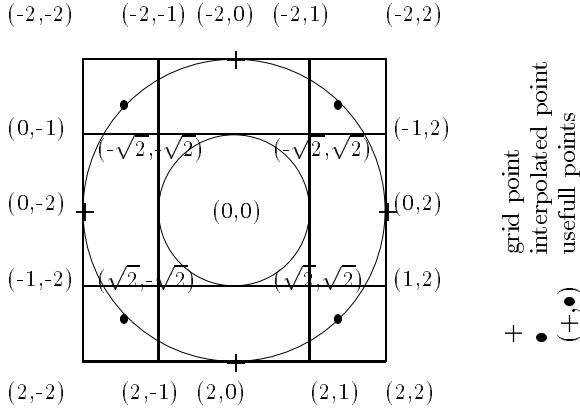


Figure 2: Circular neighbourhood of the improved model.

the models described in section 2.1 to run with a 5×5 pixel neighbourhood and similarly estimate the three additional rotation invariant parameters α_{22} , β_{22} and ζ_{22} .

The model described in eq.1 is used as starting point to estimate α_{22} and β_{22} . N_c is redefined: $N_c = \{(0, 2), (0, -2), (2, 0), (-2, 0), (\sqrt{2}, \sqrt{2}), (-\sqrt{2}, -\sqrt{2}), (\sqrt{2}, -\sqrt{2}), (-\sqrt{2}, \sqrt{2})\}$ (see Fig. 2).

The estimation of α_{22} and β_{22} is less complex in this case: one pixel intensity $y(p)$ is not depending on itself throughout the interpolated pixel intensities $y(n)$. This 5×5 pixel neighbourhood extended model has then the following final form:

$$y(p) = \alpha_{22} \cdot \sum_{n \in N'} g_n \cdot y(p+n) + \sqrt{\beta_{22}} \cdot v(p) \quad (4)$$

The new neighbourhood set N' and the new g_n coefficients are issued from the interpolation process. After calculations, we obtain:

$$\begin{aligned} g_{(-1,-1)} &= g_{(-1,1)} = g_{(1,-1)} = g_{(1,1)} = 0.2994 \\ g_{(0,-2)} &= g_{(-2,0)} = g_{(0,2)} = g_{(2,0)} = 1 \\ g_{(-2,-2)} &= g_{(-2,2)} = g_{(2,2)} = g_{(2,-2)} = 0.2117 \\ g_{(-2,-1)} &= g_{(-1,-2)} = g_{(-2,1)} = g_{(-1,2)} \\ &= g_{(2,-1)} = g_{(1,-2)} = g_{(2,1)} = g_{(1,2)} = 0.2445 \end{aligned}$$

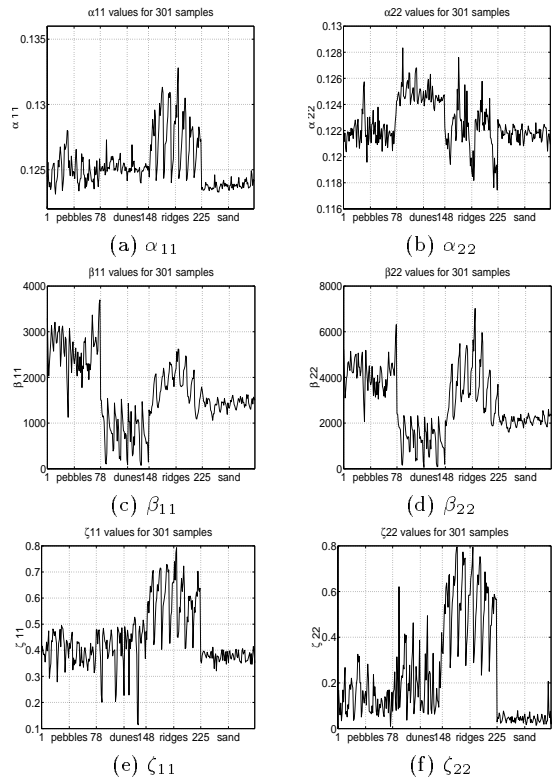


Figure 3: Values of the six rotation invariant features over 301 samples divided into four classes.

To calculate ζ_{22} , we extend the method developed to estimate ζ_{11} to $N_d = \{(0, 2), (2, 0)\}$ and then to $N_d = \{(2, 2), (-2, 2)\}$. Moreover, we introduce two other directions defined by the set of AR parameters $\{\theta_{(-1,2)}, \theta_{(2,1)}\}$ and $\{\theta_{(-2,1)}, \theta_{(1,2)}\}$. The estimation of these four AR parameters by two distinct AR models leads to the following expression for ζ_{22} :

$$\zeta_{22} = \max\{|\theta_{(2,0)} - \theta_{(0,2)}|, |\theta_{(2,2)} - \theta_{(2,-2)}|, |\theta_{(-1,2)} - \theta_{(2,1)}|, |\theta_{(-2,1)} - \theta_{(1,2)}|\} \quad (5)$$

3 FEATURE ANALYSIS

3.1 Feature appearance

We have first analyzed the behaviour of each of the six features over 301 natural 64×64 sonar images belonging to the following categories: pebbles (77), dunes (70), ridges (77) and sand (77) (see Figure 3).

We note that α_{11} and ζ_{11} (left column of Figure 3) have similar behaviours: the values of each parameter are quite identical for the pebble and dune classes; they are very high for the ridge class and very low for the sand class. Some results given in [7] for images of Brodatz album (e.g. images of pigskin, sand, wool or bubbles) show a similar behaviour between these two features as well. Features β_{11} and β_{22} are similar too. The calculation of the correlation coefficients between the six features corroborates these results (see Table 1): α_{11} and ζ_{11} are highly correlated. So are β_{11} and β_{22} as well as ζ_{11} and ζ_{22} .

3.2 Discriminant properties

The most important point to reach good classification results is the ability of some combinations of these features to separate the four considered seafloors. Figure 4 shows the

(α_{11})	1.00	0.12	0.84	0.06	0.45	0.91
(β_{11})	0.12	1.00	0.16	-0.48	0.93	0.02
(ζ_{11})	0.84	0.16	1.00	-0.14	0.44	0.83
(α_{22})	0.06	-0.48	-0.14	1.00	-0.43	0.05
(β_{22})	0.45	0.93	0.44	-0.43	1.00	0.33
(ζ_{22})	0.91	0.02	0.83	0.05	0.33	1.00

Table 1: Matrix of the correlation coefficient values calculated between the six parameters estimated over 301 images.

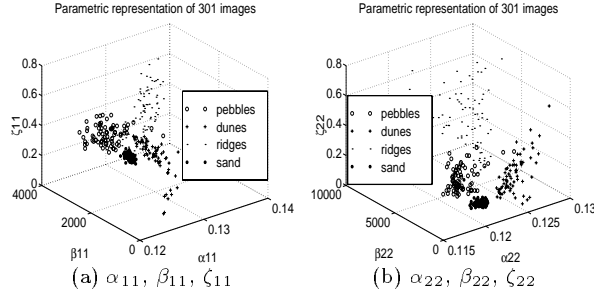


Figure 4: Parametric representations of 301 images divided into the four classes : pebbles, dunes, ridges and sand. 4(a): an image is represented by a point defined by the α_{11} , β_{11} and ζ_{11} features; 4(b): an image is represented by a point defined by the α_{22} , β_{22} and ζ_{22} features.

301 above mentioned sonar images in the space defined by $E_1 = \{\alpha_{11}, \beta_{11}, \zeta_{11}\}$ feature set (feature set issued from the basic method, see Fig. 4(a)) and by $E_2 = \{\alpha_{22}, \beta_{22}, \zeta_{22}\}$ feature set (additional feature set issued from the proposed method, see Fig. 4(b)). It is then obvious that these two sets of features can discriminate the four types of seafloors efficiently: four clusters, one for each class, are formed by these two sets. Due to correlations between some features and the discriminating power of each feature, subsets of $\{\alpha_{11}, \beta_{11}, \zeta_{11}\}$ and of $\{\alpha_{22}, \beta_{22}, \zeta_{22}\}$ may be convenient too. By visualizing graphs similar to those presented in Figure 4, we verified that $\{\alpha_{11}, \beta_{11}\}$ and $\{\alpha_{11}, \zeta_{11}\}$ were adequate feature sets as well, whereas $\{\alpha_{11}, \zeta_{11}\}$ worked poorly with pebble/dune segmentation task.

We attempted to make use of a factor analysis method (based on principal components) over the six features to reduce the feature space while increasing the discriminating power of the rotation invariant features. The results were disappointing (they were inferior or equal to those obtained without factor analysis) but not surprising mainly for the following reasons: 1) few features; 2) no non-significant features; 3) some correlations between significant features.

3.3 Rotation invariance properties

Finally we have investigated the degree of invariance of E_1 and E_2 feature sets. Figure 5 shows the discriminating power of E_1 and E_2 over a 300 sonar image database (called *rotated database*) which was obtained as follows : one 512×768 image was chosen for each class; each of them was rotated with angles of rotation from 10° up to 80° with steps 10° plus 120° and 150° angles; each of these rotated images per class was segmented into 64×64 images and some were selected to form the *rotated database*. We note that the clusters are well-formed too although they look slightly less separable than those represented on Figure 4, probably due to the isolated point (see Figure 5).

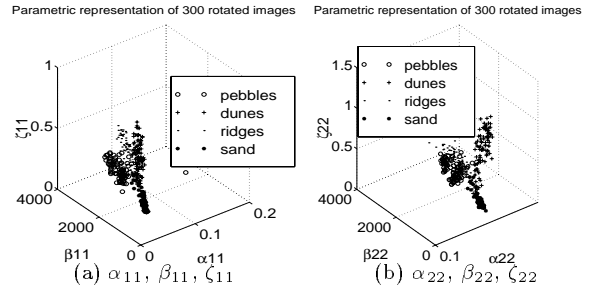


Figure 5: Parametric representations of 300 rotated images divided into the four classes : pebbles, dunes, ridges and sand. 5(a): an image is represented by a point defined by the α_{11} , β_{11} and ζ_{11} features; 5(b): an image is represented by a point defined by the α_{22} , β_{22} and ζ_{22} features.

All the analyses presented in this section demonstrate that all the features issued from the basic model (see section 2.1) and those issued from the proposed improved model (see section 2.2) are appropriate to discriminate the four types of considered seafloors.

4 CLASSIFICATION RESULTS

In this section, performances of the three feature sets E_1 , E_2 and $E_3 = E_1 \cup E_2$ are evaluated through a neural classifier (MLP) with one hidden layer. Classification results are also given for a K-Nearest Neighbour Algorithm (called K-NNA) for comparison (the K-NNA requires about ten more multiplications than the MLP). Previous experimental tests have provided best results for an MLP with ten hidden neurons and for a K-NNA with $K=10$. Two training and test databases are used to perform identification tasks. *Database_Lrn1* and *database_test1*, the learning- and associated test- base, are used to evaluate the discriminant property of the three considered feature sets: the 301 samples of *database_Lrn1* represent images (the same as those used to analyze parameter behaviours, see Figure 3) with the same orientation as the 288 images represented by samples of *database_test1*. *Database_Lrn2* and *database_test2* are used to evaluate the rotation invariant nature of the three feature sets. Samples of *database_Lrn2* are issued from images having different orientations (rotated images with relative angles of 10° , 20° , 30° , 40° and 50°) from the images represented by samples of *database_test2* (rotated images with relative angles of 60° , 70° , 80° , 120° and 150°). Classification results of Table 2 (obtained on *database_test1*) show that performances are the same with MLP and K-NNA. Furthermore, feature set E_2 performs quite better than E_1 which performs very poorly for ridge recognition. It is also obvious that combination of feature sets E_1 and E_2 does not produce better results than E_2 alone. This is probably due to the existence of high correlations between the features (remember Tab. 1). The results summarized in Table 3 (obtained on *Database_test2*) confirm that the proposed improved method performs better than the one described in section 2.1.

Comparative study has finally been conducted. The compared method is a rotation invariant version of the Grey Level Cooccurrence Method (GLCM) [5]. Cooccurrence matrices are calculated for distances d of 1, 2, 3 and 4 and for directions θ of 0° , 45° , 90° and 135° . Selected features are *ASM* (Angular Second Moment), *CON* (Contrast), *COR*

Recognition Rates in %						
		PE	DU	RI	SA	GLOBAL
E_1	MLP	98	87	68	100	88
	K-NNA	98	94	61	100	87
E_2	MLP	98	100	94	92	96
	K-NNA	97	100	93	95	96
E_3	MLP	98	97	90	100	96
	K-NNA	98	100	90	100	97

Table 2: Evaluation of feature’s relevance. Recognition rates obtained with two classifiers for the three feature sets E_1 , E_2 and E_3 and for the four classes PEbbles, DUNes, RIdges and SAnd. Learning set (resp. testing set) is *database_lrn1* (resp. *database_test1*).

Recognition Rates in %						
		PE	DU	RI	SA	GLOBAL
E_1	MLP	100	56	93	100	87
	K-NNA	100	52	94	100	86
E_2	MLP	100	74	100	100	93
	K-NNA	97	73	100	100	92
E_3	MLP	100	62	100	100	90
	K-NNA	100	64	100	100	91

Table 3: Evaluation of feature’s invariance. Recognition rates obtained with two classifiers for the three feature sets E_1 , E_2 and E_3 and for the four classes PEbbles, DUNes, RIdges and SAnd. Learning set (resp. testing set) is *database_lrn2* (resp. *database_test2*).

Recognition Rates in %						
		PE	DU	RI	SA	GLOBAL
GLCM		100	66	100	100	90
E_2		100	74	100	100	93

Table 4: Recognition rates obtained with a MLP classifier, for the GLCM method and the E_2 feature set, for the four classes PEbbles, DUNes, RIdges and SAnd. Learning set (resp. testing set) is *database_lrn2* (resp. *database_test2*).

(Correlation) and ENT (Entropy). To make these features rotation invariant, we take the mean and the standard deviation of each feature, calculated over the four directions for a given distance. Thus, 32 parameters are considered. Comparative results are given in Table 4. The improved rotation invariant method performs as well as GLCM for the identification of sand, ridge (strongly directional) and pebble seafloors and a little better for dune identification. Furthermore, the rotation invariant method produces a reduced set of relevant features. So it is much more effective. Due to its only three features required, the extraction process is computationally less expensive and so is the training stage.

5 CONCLUSIONS

Through this study, we have first shown that the rotation invariant autoregressive method, developed a few years ago, could be successfully applied to natural noisy sidescan sonar images (with multiplicative noise). We have proposed an improvement of this method which theoretically better describes the spatial dependencies as well as the orientation of the textures. We have demonstrated on four types of

seafloors that the proposed approach performs better than the basic method and slightly better than the GLCM, with the advantage over the latter of providing a very compact parameter set.

References

- [1] H. DERIN and H. ELLIOT. Modeling and segmentation of noisy and textured images using gibbs random fields. *IEEE Transactions on pattern analysis and machine intelligence*, PAMI-9(1):39–55, january 1987.
- [2] M.M. GALLOWAY. Texture analysis using gray level run lengths. Technical report, Maryland University, College Park, MD, USA, july 1974.
- [3] G.M. HALEY and B.S. MANJUNATH. Rotation-invariant texture classification using modifier GABOR filters. *ICIP’95*, pages 262–265, 23-26 october 1995. Washington.
- [4] R.M. HARALICK. Statistical and structural approaches to texture. *Proceedings of the IEEE*, 67(5), may 1979.
- [5] R.M. HARALICK, K. SHANMUGAM, and ITS’HAK DI-ENSTEIN. Textural features for image classification. *IEEE Trans. Syst., Man, Cybern.*, SMC-3:610–621, november 1973.
- [6] R.L. KASHYAP, R. CHELLAPPA, and A. KHOTANZAD. Texture classification using features derived from random field models. *Pattern Recognition Letters*, 1(1):43–50, october 1982.
- [7] R.L. KASHYAP and A. KHOTANZAD. A model-based method for rotation invariant texture classification. *IEEE Trans. Pattern Anal. and Machine Intell.*, PAMI-8(4):472–481, july 1986.
- [8] J. MAO and ANIL K. JAIN. Texture classification and segmentation using multiresolution simultaneous autoregressive models. *Pattern Recognition*, 25(2):173–188, Februar 1992.
- [9] D.J. MARCEAU, P.J. HOWARTH, J.M.M. DUBOIS, and D.J. GRATTON. Evaluation of the grey-level cooccurrence matrix method for land cover classification using SPOT imagery. *IEEE Transactions on Geoscience and Remote Sensing*, 28(4):513–519, july 1990.
- [10] R. PORTER and N. CANAGARAJAH. Robust rotation invariant texture classification. *ICASSP’97*, IV:3157–160, 21-24 april 1997. Munich, Germany.
- [11] E. SALI and H. WOLFSON. Texture classification in aerial photographs and satellite data. *Int. J. of Remote Sensing*, 13(18):3395–408, december 1992.
- [12] W.K STEWART, M. JIANG, and M. MARRA. A neural network approach to classification of sidescan sonar imagery from a midocean ridge area. *IEEE Journal of Oceanic Engineering*, 19(2):214–224, april 1994.
- [13] S. SUBRAMANIAM, H. BARAD, and A.B. MARTINEZ. Seafloor characterization using texture. *Proceedings IEEE Southeastcon’93*, 1993. Charlotte, NC, USA.
- [14] H. THOMAS, C. COLLET, G. BUREL, and K. YAO. Classification neuronale des fonds marins par modelisation autoregressive bidimensionnelle. *GRETSI’97*, pages 925–928, septembre 1997. National Conference on Signal and Image Processing, Grenoble, France.
- [15] M. TUCERYAN and ANIL K. JAIN. *Texture analysis*, chapter 2.1, pages 235–276. in Handbook of Pattern Recognition and Computer Vision, 1993. Eds. C.H. CHEN, L.F. PAU and P.S.P. WANG, World Scientific Publishing Company.

Acknowledgement

The authors thank the GESMA (Groupe d’Etudes Sous-Marines de l’Atlantique) for having provided us with the studied sonar images.